

Evidence for Dopamine Abnormalities in the Substantia Nigra in Cocaine Addiction Revealed by Neuromelanin-Sensitive MRI

Clifford M. Cassidy, Ph.D., Kenneth M. Carpenter, Ph.D., Anna B. Konova, Ph.D., Victoria Cheung, B.Sc., Alexander Grasseti, B.A., Luigi Zecca, M.D., Ph.D., Anissa Abi-Dargham, M.D., Diana Martinez, M.D., Guillermo Horga, M.D., Ph.D.

Objective: Recent evidence supports the use of neuromelanin-sensitive MRI (NM-MRI) as a novel tool to investigate dopamine function in the human brain. The authors investigated the NM-MRI signal in individuals with cocaine use disorder, compared with age- and sex-matched control subjects, based on previous imaging studies showing that this disorder is associated with blunted presynaptic striatal dopamine.

Methods: NM-MRI and T₁-weighted images were acquired from 20 participants with cocaine use disorder and 35 control subjects. Diagnostic group effects in NM-MRI signal were determined using a voxelwise analysis within the substantia nigra. A subset of 20 cocaine users and 17 control subjects also underwent functional MRI imaging using the monetary incentive delay task, in order to investigate whether NM-MRI signal was associated with alterations in reward processing.

Results: Compared with control subjects, cocaine users showed significantly increased NM-MRI signal in ventrolateral

regions of the substantia nigra (area under the receiver operating characteristic curve=0.83). Exploratory analyses did not find a significant correlation of NM-MRI signal to activation of the ventral striatum during anticipation of monetary reward.

Conclusions: Given that previous imaging studies show decreased dopamine signaling in the striatum, the finding of increased NM-MRI signal in the substantia nigra provides additional insight into the pathophysiology of cocaine use disorder. One interpretation is that cocaine use disorder is associated with a redistribution of dopamine between cytosolic and vesicular pools, leading to increased accumulation of neuromelanin. The study findings thus suggest that NM-MRI can serve as a practical imaging tool for interrogating the dopamine system in addiction.

Am J Psychiatry 2020;177:1038–1047; doi:10.1176/appi.ajp.2020.20010090

Alterations of dopamine function have been demonstrated in cocaine use disorder using positron emission tomography (PET), including measures of dopamine uptake, receptor density, and dopamine release (1). The reduction of stimulant-induced presynaptic dopamine release in cocaine users, measured with PET, is well replicated (1–4) and is associated with more refractory symptoms of cocaine use disorder, including relapse (1, 2). However, while PET can provide important insights on dopamine signaling in addiction, it is costly and requires significant specialized infrastructure. Furthermore, its use in longitudinal studies and research in younger, at-risk populations is limited by the risks of radioactivity exposure.

Recent work suggests that neuromelanin-sensitive MRI (NM-MRI) may provide a complementary noninvasive proxy measure of dopamine function and integrity (5, 6). Neuromelanin

(NM) is a pigment generated from the conversion of cytosolic dopamine that accumulates gradually over the lifespan in dopamine neurons of the substantia nigra (SN) (7). NM is bound to iron, forming paramagnetic complexes that can be imaged using MRI (6, 8, 9). NM-MRI can reliably capture NM depletion following SN neurodegeneration in Parkinson's disease (6, 10). Critically, this technique can also capture alterations in dopamine function in the absence of neurodegeneration (5, 11), consistent with *in vitro* evidence that stimulating dopamine synthesis boosts NM synthesis (12, 13).

In particular, our recent work showed that NM-MRI signal within a subregion of the SN is increased in relation to psychosis (5), consistent with PET findings of increased dopamine signaling in psychosis (14). We further showed that NM-MRI signal correlates directly with both PET measures

See related features: **Editorial** by Dr. Bradberry (p. 1019) and **Video** by Dr. Pine (online)

of presynaptic dopamine release and resting blood flow in the midbrain (5). Thus, this work demonstrates that NM-MRI provides a proxy measure for functional changes in dopaminergic pathways, with utility for studying psychiatric disorders in the absence of overt neurodegeneration.

Here, we sought to employ NM-MRI to examine whether similar changes could be detected in cocaine use disorder, a disorder involving dopamine dysfunction. To this end, our main analyses tested for effects of diagnostic group (individuals with and without cocaine use disorder) on NM-MRI signal in the SN. Our hypothesis, based on previous PET studies (1, 3), was that cocaine use disorder would be associated with reduced NM-MRI signal. In exploratory analyses, we then evaluated associations between changes in NM-MRI signal intensity in cocaine use disorder and hemodynamic brain responses during the monetary incentive delay task. Activation of the ventral striatum during the anticipation of reward in this task has been shown to provide a robust functional readout of reward processing (15) related to dopamine (16, 17) that is consistently reduced in drug and behavioral addictions (18, 19). Since the ventral striatum receives projections from the ventral tegmental area and the dorsomedial SN (20, 21), we explored the relationship between NM-MRI signal in the SN and reward-related activation in the ventral striatum.

METHODS

Participants

This study was approved by the Institutional Review Board of the New York State Psychiatric Institute. All participants provided written informed consent. The cocaine-using participants met DSM-5 criteria for moderate to severe cocaine use disorder with no other current psychiatric diagnosis or current medical illness. Any other substance use disorder (aside from tobacco) was an exclusion criterion. At the time of study entry, the cocaine-using participants were actively using smoked cocaine, which was verified by urine toxicology (using a test strip with a threshold of 300 ng/mL). Despite being active users, they were required to be abstinent from cocaine for 5 days prior to the scan, which was verified by urine drug testing (dipstick, performed every other day). Participants refrained from tobacco use for at least 1 hour before scanning. A group of tobacco-using and non-tobacco-using control subjects was also included. Screening procedures included a physical examination, ECG, and laboratory tests. All participants were recruited through advertisements and by word of mouth. Control subjects were excluded if they had a current or past psychiatric disorder (except tobacco use disorder), a history of neurological disorders, or any current major medical illness. In total, 58 men participated in the study. Three participants (one cocaine user and two control subjects) were excluded because of unusable NM-MRI images (two participants because of motion during scanning [showing clearly visible smearing or banding artifacts affecting the midbrain] and one because of incorrect image-stack placement). Thus, a total of 55 participants were

retained for analysis: 20 cocaine users and 35 age- and sex-matched control subjects (Table 1). All participants completed self-report questionnaires, including the Multidimensional Scale of Perceived Social Support (22) and the Beck Depression Inventory (23).

NM-MRI Acquisition

MR images were acquired for all study participants on a GE Healthcare 3-T MR750 scanner using a 32-channel phased-array Nova head coil following the methods used in our previous study (5). For logistical reasons, a few scans (four of the 55 scans, or 7%) were acquired using an eight-channel InVivo head coil instead. NM-MRI images were acquired using a two-dimensional gradient recalled echo sequence with magnetization transfer contrast with the following parameters: TR=260 ms; TE=2.68 ms; flip angle=40°; in-plane resolution=0.39×0.39 mm²; partial brain coverage, with FOV=162×200; matrix=416×512; number of slices=10; slice thickness=3 mm; slice gap=0 mm; magnetization transfer frequency offset=1,200 Hz; number of excitations=8; acquisition time=8.04 minutes. The slice-prescription protocol consisted of orienting the image stack along the anterior commissure–posterior commissure line and placing the top slice 3 mm below the floor of the third ventricle (for more detail, see reference 5). This protocol provided coverage of SN-containing portions of the midbrain and surrounding structures. To support the preprocessing of NM-MRI images (see below), whole brain high-resolution T₁-weighted structural MRI scans were also acquired using a fast spoiled gradient echo sequence (inversion time=500 ms, TR=6.37 ms, TE=2.59 ms, flip angle=11°, FOV=256×256, number of slices=244, isotropic voxel size=1.0 mm³) or, in some cases, a three-dimensional BRAVO sequence (inversion time=450 ms, TR≈7.85 ms, TE≈3.10 ms, flip angle=12°, FOV=240×240, number of slices=220, isotropic voxel size=0.8 mm³). Quality of NM-MRI images was visually inspected for artifacts immediately after acquisition, and scans were repeated when necessary, time permitting.

NM-MRI Preprocessing

As in our previous work (5), NM-MRI scans were preprocessed using SPM12 to allow for voxelwise analyses in standardized Montreal Neurological Institute (MNI) space. NM-MRI scans were first coregistered to participants' T₁-weighted scans. Tissue segmentation was then performed using the T₁-weighted images. NM-MRI scans were normalized to MNI space using DARTEL routines with a gray- and white-matter template generated from all study participants. The resampled voxel size of unsmoothed, normalized NM-MRI scans was 1 mm, isotropic. All images were visually inspected after each preprocessing step. Intensity normalization and spatial smoothing were then performed using custom MATLAB (MathWorks, Natick, Mass.) scripts. Contrast-to-noise ratio (CNR) for each participant and voxel v was calculated as the relative difference in NM-MRI signal intensity I from a reference region RR of white matter tracts known to have minimal NM content, the crus cerebri, as follows:

TABLE 1. Demographic and clinical characteristics of participants in a neuromelanin-sensitive MRI study of cocaine use disorder^a

Characteristic	Control Subjects (N=35)		Cocaine Users (N=20)		p
	N	%	N	%	
Race/ethnicity					0.08
African American	14	40	15	75	
Caucasian	5	14	2	10	
Hispanic	4	11	3	15	
Other	7	20	0	0	
Tobacco user	13	37	15	75	0.011
Occasional alcohol use	14	82	16	84	1
Occasional cannabis use	3	18	9	47	0.08
	Mean	SD	Mean	SD	p
Age (years)	45.1	10.2	47.3	8.1	0.41
Body mass index	26.0	3.8	27.3	2.5	0.23
Education (years)	14.3	1.8	12.4	1.29	<0.001
Perceived social support (MSPSS score)	70.9	7.5	60.6	15.2	0.014
Depressive symptoms (BDI score)	1.2	1.8	7.5	8.8	0.005
Cigarettes per day (tobacco users only)	8.9	5.7	5.9	2.2	0.01
Duration of cocaine use (years)			21.9	9.3	
Dollars spent per week on cocaine ^b			207	138	

^a Reported p values are from t tests for continuous measures and chi-square or Fisher's tests for tests of proportions. BDI=Beck Depression Inventory; MSPSS=Multidimensional Scale of Perceived Social Support.

^b Average amount of money spent per week on cocaine is used as a proxy for amount of use. Cocaine cost approximately \$30/g in the New York City area at the time the data were being collected.

$$CNR_v = (I_v - mode(I_{RR}))/mode(I_{RR})$$

A template mask of the reference region and of the SN was created by manual tracing on a template NM-MRI image in MNI space (an average of normalized NM-MRI scans from all study participants; see Figure 1 and our previous report for more details [5]). The $mode(I_{RR})$ was calculated for each participant from a kernel-smoothing-function fitted to a histogram of the distribution of all voxels in the mask. The resulting NM-MRI contrast-to-noise ratio maps were then spatially smoothed with a 1-mm full width at half maximum Gaussian kernel.

NM-MRI Analysis

All analyses were carried out in MATLAB. Following the methods used in our previous study (5), our main analysis consisted of a voxelwise analysis of contrast-to-noise ratio values in the SN mask. This approach captures topographic alterations presumably corresponding with functionally distinct SN neuron subpopulations (20) and which previously showed high sensitivity to dopaminergic pathophysiology (5). In particular, the primary voxelwise analysis examined specific differences between cocaine users and control subjects via a robust linear regression analysis (the *robustfit* function in MATLAB) that predicted contrast-to-noise ratio (NM signal) at every voxel v within the SN mask as follows:

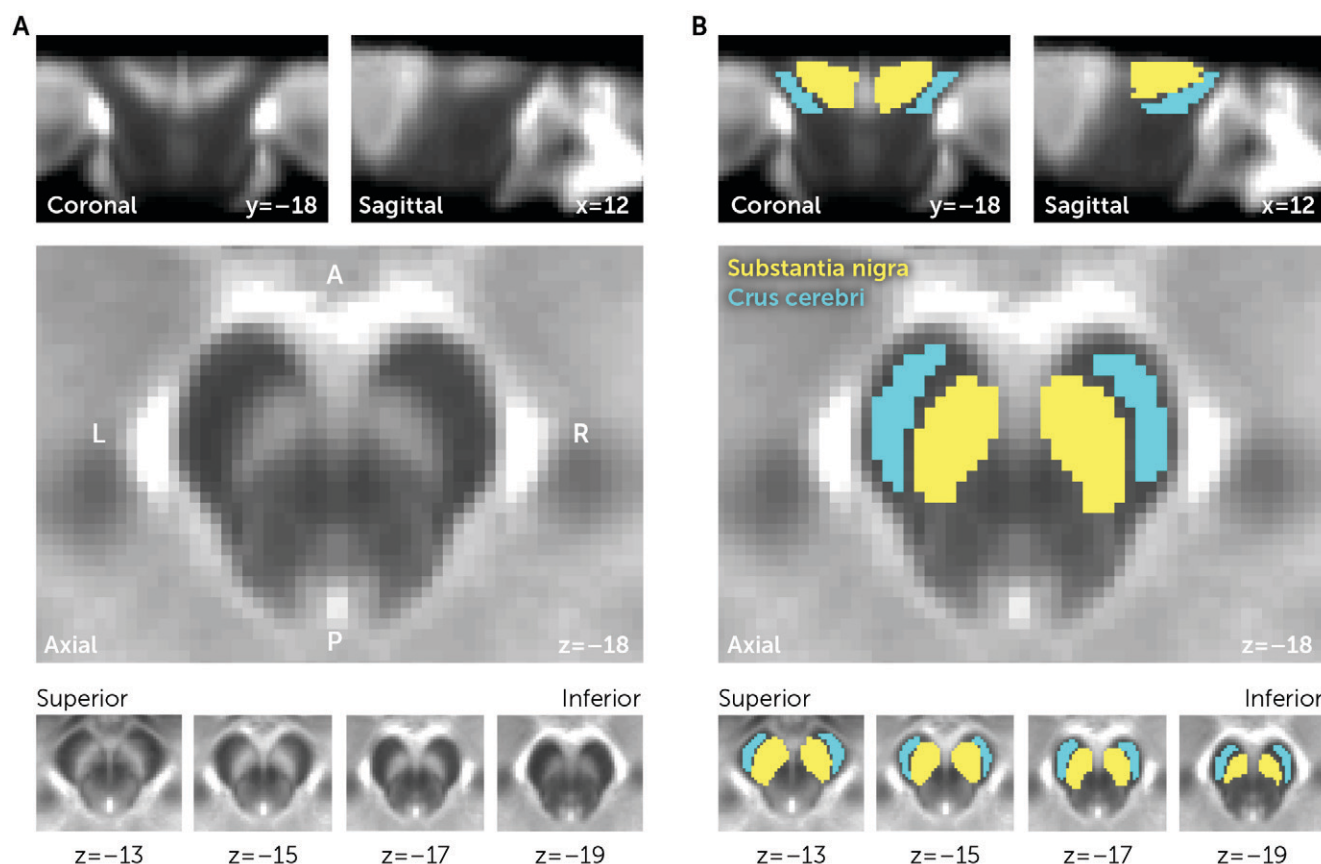
$$CNR_v = \beta_0 + \beta_1 \cdot diagnosis + \sum_{i=2}^n \beta_i \cdot nuisance\ covariate + \epsilon$$

with tobacco use (cigarettes per day), head coil, and age as nuisance covariates. Note that correcting for age is critical given the known relationship between age and NM accumulation (7). As in our previous work (5), we used a group-derived template SN mask after censoring participant data points with missing values because of incomplete SN coverage or extreme values (contrast-to-noise ratio < -8% or contrast-to-noise ratio >40%; on average, 71 voxels [SD=195] or 4% of all SN voxels were censored per subject). To correct for multiple comparisons, again following the methods of our previous work (5), we defined the spatial extent of an effect as the number of voxels k (adjacent or nonadjacent) exhibiting differences between cocaine users and control subjects in NM signal in either the positive or the negative direction (voxel-level height threshold for t test of regression coefficient β_1 of $p < 0.05$, one-sided; note that our results remained significant at a more stringent height threshold of $p < 0.01$). Significance testing was then determined on the basis of a permutation test in which diagnosis labels (cocaine users, control subjects) were randomly shuffled with respect to individual maps of NM signal. This provided a measure of spatial extent for each of 10,000 permuted data sets, forming a null distribution against which to calculate the probability of observing the spatial extent k of the effect in the true data by chance. Thus, this test corrects for multiple comparisons by determining whether an effect's spatial extent k was greater than would be expected by chance (corrected $p < 0.05$; 10,000 permutations).

For a more detailed topographical description of the voxelwise effects in the SN, a post hoc multiple linear regression analysis across SN voxels was used to predict the strength of an effect as a function of MNI voxel coordinates in the x (absolute distance from the midline), y, and z directions within the SN mask. For completeness, we also carried out a region-of-interest analysis on the average NM signal across the whole SN mask. This region-of-interest analysis consisted of a robust linear regression analysis including head coil, age, and incomplete SN coverage (yes/no) as nuisance covariates.

The ability of NM-MRI to segregate participants by diagnostic group was determined by calculating effect size

FIGURE 1. Masks of the reference region and of the substantia nigra in an NM-MRI study of cocaine use disorder^a



^a Panel A is the template of the midbrain in MNI space created by averaging spatially normalized neuromelanin-sensitive MRI (NM-MRI) images from all participants. The substantia nigra (SN) is clearly visible as a hyperintense region. In panel B, a mask of the SN (yellow; an overinclusive mask to ensure full SN coverage for all participants) and the crus cerebri reference region (cyan) in MNI space was traced on the NM-MRI template and applied to all participants for calculation of contrast-to-noise ratio.

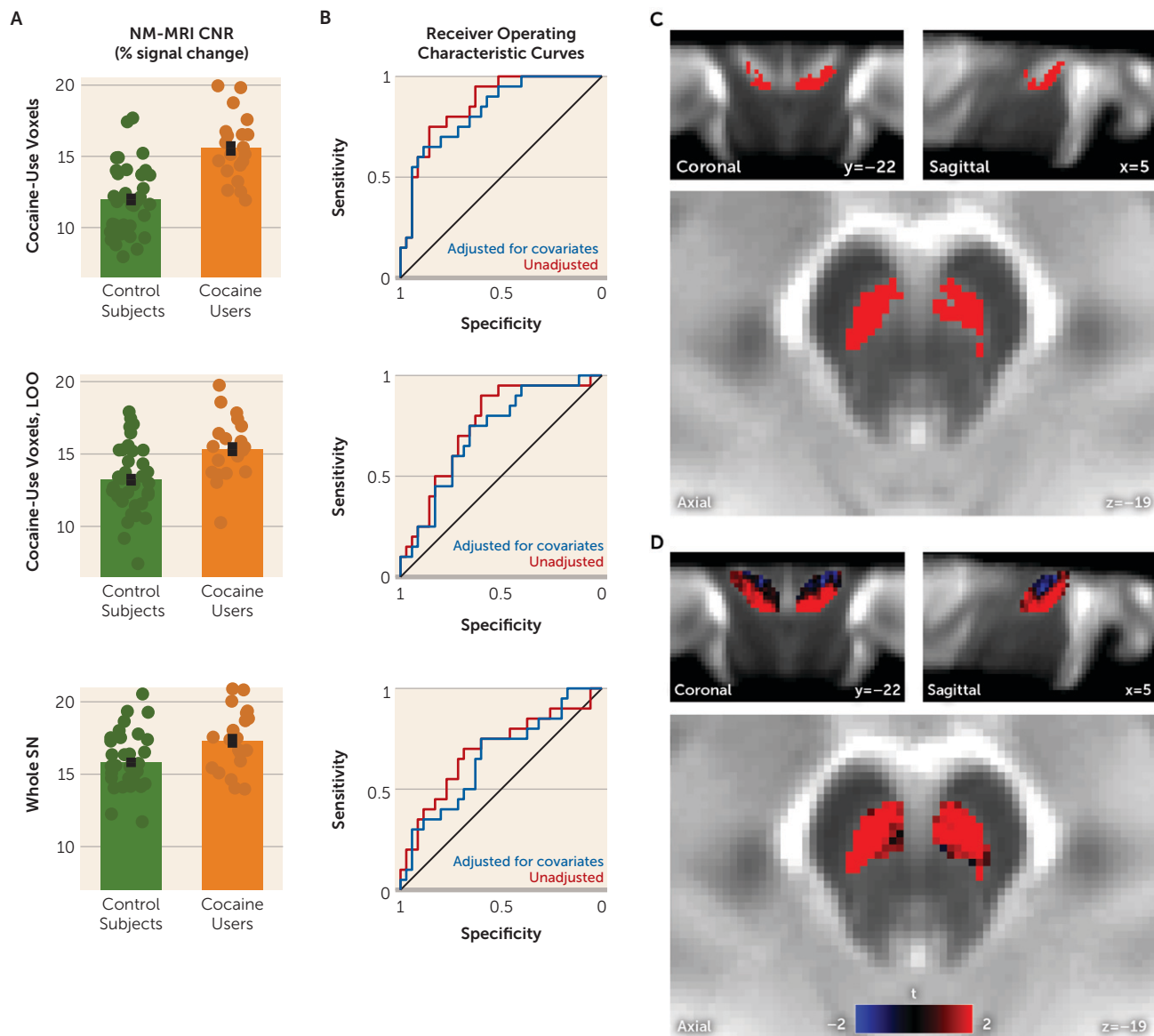
estimates and area under the receiver operating characteristic curve based on the mean NM-MRI signal in voxels identified in the primary voxelwise analysis to be relevant to cocaine use disorder (henceforth referred to as “cocaine-use voxels”)—voxels showing a diagnosis effect via the primary voxelwise analysis or via a voxelwise analysis following a leave-one-out procedure. The leave-one-out procedure was employed to obtain a measure of effect size unbiased by voxel selection: for a given participant, voxels for which the variable of interest was related to NM-MRI signal were first identified in an analysis including all participants except for this (held-out) participant. The mean signal in the held-out participant was then calculated from this set of voxels. This procedure was repeated for all participants, so that each participant had an extracted mean NM-MRI signal value obtained from an analysis that excluded them. Confidence intervals for Cohen’s *d* and *f*² effect size measures were determined by bootstrapping.

Partial correlations related clinical measures to NM-MRI signal extracted from cocaine-use voxels, with age and tobacco use as covariates. Partial (nonparametric) Spearman correlation was used because the clinical measures were not normally distributed according to a Lilliefors test at $p < 0.05$.

fMRI Methods

fMRI data were collected in 37 of the study participants (20 cocaine users, 17 control subjects). Blood-oxygen-level-dependent (BOLD) fMRI was acquired while participants completed the monetary incentive delay task. Echo planar images were acquired with the following parameters: TR=1,500 ms; TE=27 ms; flip angle=60°; in-plane resolution=3.5×3.5 mm²; slice thickness=4 mm; slice gap=1 mm. There were two runs, each lasting 12.1 minutes. fMRI images were preprocessed using standard methods in SPM12, including slice-time correction, realignment, coregistration to the T₁-weighted scans, spatial normalization to standardized MNI space, and smoothing (6 mm full width at half maximum kernel). The monetary incentive delay task employed was similar to a standard version (24) involving presentation of visual cues (geometric shapes) linked to subsequent receipt of feedback regarding monetary reward (\$1 or \$5), monetary loss (\$1 or \$5), or no outcome (\$0). The task consisted of 110 trials equally divided into the five conditions. Earning money or avoiding losses was probabilistically achieved by having participants make fast key presses after the visual cue. The time available to make a key press was personalized according to participants’ motor

FIGURE 2. Results of NM-MRI signal analysis in the substantia nigra in a study of cocaine use disorder^a



^a Panel A shows group differences in neuromelanin-sensitive MRI (NM-MRI) signal between cocaine users and control subjects. The scatterplots show extracted NM-MRI signal (contrast-to-noise ratio, CNR) averaged within cocaine-use voxels (top graph; defined in panel C), cocaine-use voxels as defined with a leave-one-out (LOO) procedure (middle graph), and the whole substantia nigra (SN) (bottom graph). To complement results showing the effect of diagnostic group on NM-MRI signal after adjusting for covariates (see panel B and statistics reported in the text), these scatterplots show diagnostic group differences in the raw, unadjusted NM-MRI signal. Error bars indicate standard error of the mean. Panel B shows receiver operating characteristic curves displaying sensitivity and specificity of the NM-MRI signal in separating diagnostic groups based on signal extracted from cocaine-use voxels (top graph), cocaine-use voxels defined with a leave-one-out procedure (middle graph), and whole SN (bottom graph). The blue line represents NM-MRI signal adjusted for age, head coil, and tobacco use covariates; the red line represents unadjusted NM-MRI signal. Panel C is a map of voxels in which cocaine users exhibited higher NM-MRI signal than control subjects (shown in red) (robust linear regression, $p < 0.05$ one-sided). This set of voxels was above chance level (corrected $p = 0.025$, permutation test). Panel D shows unthresholded results of the same analysis showing the t-statistic for the diagnostic group effect for all SN voxels. Voxels where NM-MRI signal was higher in the cocaine users are shown in red, and voxels where the signal was lower in cocaine users are shown in blue.

speed during practice testing. A first-level model included boxcar regressors for all five conditions during the anticipation period (defined as the period following button pressing and prior to feedback), the prospect period (following cue presentation and prior to button pressing), and the outcome period (when feedback was delivered). Nuisance regressors included 24 motion parameters (six motion

parameters and their squares, derivatives, and squared derivatives) and session-specific intercepts corresponding to the two runs. As in previous work (15), activation during reward anticipation was defined by the contrast between the \$5 and \$0 gain conditions. For each participant, we extracted the signal from this contrast within a mask of the ventral striatum (from a publicly available functional mask

of the striatum; <https://osf.io/jkzwp/>). The ventral striatum is the brain structure most commonly investigated when using this task (19), and it has been shown to provide a robust and reliable readout of reward-related activity during the task (25). To determine relationship to NM-MRI, a linear regression was used to investigate the effect of diagnosis, NM-MRI signal in cocaine-use voxels, and the interaction of diagnosis by NM-MRI signal on anticipatory BOLD activity in the ventral striatum, controlling for age and tobacco use.

RESULTS

Effect of Diagnosis on NM-MRI Signal in the Substantia Nigra

A priori voxelwise analysis of differences between cocaine users and control subjects. A subset of voxels located mostly ventrolaterally within the SN exhibited significantly increased NM-MRI signal (contrast-to-noise ratio) in cocaine users compared with control subjects (344 of 1,775 voxels at $p < 0.05$, robust linear regression controlling for age, head coil, and cigarettes per day; corrected $p = 0.025$, permutation test; peak voxel MNI coordinates [x, y, z]: 6, -26, -17 mm) (Figure 2C). Detailed topographical analyses of this effect are presented in Table S1 in the online supplement. In this sample of relatively light smokers, tobacco use was not significantly associated with differences in NM-MRI signal (267 SN voxels exhibited signal that positively correlated with cigarettes per day in the primary linear regression model; corrected $p = 0.054$).

Based on the average NM-MRI signal values extracted from the voxels in which cocaine users showed increased NM-MRI signal relative to control subjects in the voxelwise analysis (cocaine-use voxels, shown in red in Figure 2C, with extracted values from these voxels shown in Figure 2A top panel), a diagnosis of cocaine use disorder had a moderate to large effect on NM-MRI signal (Cohen's $d = 1.34$, 95% CI = 0.91, 1.90, Cohen's $f^2 = 0.46$, 95% CI = 0.19, 0.95; unbiased leave-one-out Cohen's $d = 0.77$, 95% CI = 0.35, 1.27, Cohen's $f^2 = 0.15$, 95% CI = 0.02, 0.43; all estimates based on NM-MRI signal adjusted for age, head coil, and tobacco use). Diagnostic differences in adjusted NM-MRI signal extracted from cocaine-use voxels remained moderate to large when analyzing subsets of the study sample to address possible confounders (controlling for years of education: Cohen's $d = 0.76$, 95% CI = 0.22, 1.39, $N = 38$; controlling for depressive symptoms: Cohen's $d = 0.84$, 95% CI = 0.31, 1.52, $N = 37$; controlling for perceived social support: Cohen's $d = 1.06$, 95% CI = 0.52, 1.72, $N = 37$; excluding non-tobacco users: Cohen's $d = 1.05$, 95% CI = 0.50, 1.74, $N = 28$; excluding participants scanned with eight-channel coil: Cohen's $d = 1.38$, 95% CI = 0.9, 1.97, $N = 51$). Furthermore, most cocaine users could be successfully classified relative to all 35 control subjects on the basis of adjusted NM-MRI signal extracted from cocaine-use voxels (area under the receiver operating characteristic curve [AUC] = 0.83, unbiased leave-one-out AUC = 0.71) (Figure 2B).

For completeness, we also examined NM-MRI signal averaged within the whole SN using a region-of-interest analysis. Here again, cocaine users showed significantly increased NM-MRI signal compared with control subjects ($t = 2.07$, $df = 49$, $p = 0.044$, Cohen's $d = 0.62$, 95% CI = 0.19, 1.12, robust linear regression controlling for age, head coil, tobacco use, and incomplete SN coverage; AUC = 0.69).

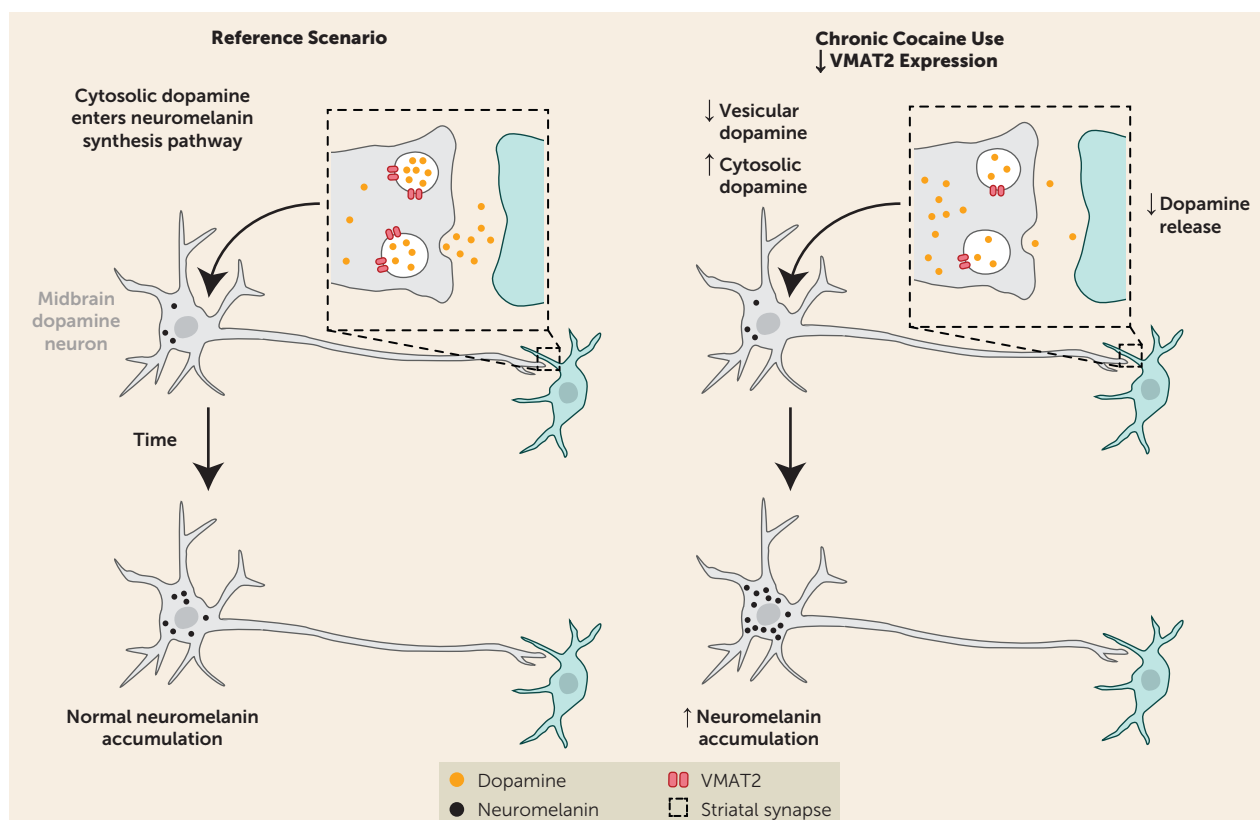
Exploratory analysis of the relationship between NM-MRI signal in SN and measures of cocaine use severity. We tested whether the NM-MRI signal extracted from cocaine-use voxels correlated with severity of cocaine use and found no significant correlation with duration of use ($\rho = -0.33$, $p = 0.18$) or dollars spent per week on cocaine ($\rho = -0.08$, $p = 0.74$; partial Spearman correlations controlling for age and tobacco use).

Exploratory analysis of the relationship between NM-MRI signal in SN and ventral striatum response to reward anticipation. To investigate the relationship of the NM-MRI findings to dopamine-related circuit dysfunction in cocaine use disorder, we measured fMRI BOLD activation in the ventral striatum during anticipation of monetary reward. As expected, across all participants, BOLD signal was higher in the ventral striatum when anticipating reward compared with no reward ($t = 2.56$, $df = 36$, $p = 0.015$, one-sample t test of \$5-to-\$0 contrast during anticipation). But this reward-related activation in the ventral striatum did not differ between the groups ($\beta = 0.038$, $t = 0.72$, $df = 32$, $p = 0.48$) or correlate with NM-MRI signal in cocaine-use voxels across all participants ($\beta = -0.015$, $t = -1.52$, $df = 32$, $p = 0.14$). There was also no group-by-NM-MRI signal interaction on reward-related activation in the ventral striatum ($p = 0.24$; linear regression controlling for age and tobacco use).

DISCUSSION

We have presented data showing increased NM-MRI signal in the SN of individuals with cocaine use disorder. This increase was not present throughout the whole SN but rather predominated in more ventral and lateral SN subregions. Given that the NM-MRI signal reflects the concentration of synthetic melanins in experimental preparations (8) and of NM in postmortem midbrain tissue (5), and that NM accumulation in the SN depends on dopamine function (5, 12, 13), these findings suggest that cocaine users exhibit elevated NM concentration in these SN subregions that may be indicative of dopaminergic dysfunction.

Our finding of elevated NM signal in cocaine users was surprising given the previous PET studies showing that presynaptic dopamine is blunted in cocaine use disorder (1-4). However, this discrepancy provides additional insight into the pathophysiology of dopamine signaling in this disorder. The combination of blunted dopamine release in the striatum and elevated NM in the SN suggests that dopamine is distributed differently in cocaine users compared with control subjects. Less dopamine concentrated in synaptic

FIGURE 3. Schematic of the hypothesized redistribution of dopamine between vesicular and cytosolic stores in the substantia nigra in cocaine use disorder^a

^a The schematic depicts trafficking of dopamine between the cytosolic, vesicular, and synaptic pools in the striatum and subsequent accumulation of neuromelanin in the substantia nigra (curved arrow) in healthy subjects (reference scenario) and in individuals with cocaine use disorder (chronic cocaine use). Boxes with dashed lines show a schematic detail of the striatal synapse between the presynaptic dopamine neuron (gray) and the postsynaptic striatal neuron (green). In the reference scenario on the left, the cytosolic dopamine pool is normally converted to neuromelanin and accumulates gradually over the lifespan in the cell bodies of presynaptic dopamine neurons within the substantia nigra in the midbrain. The theoretical chronic cocaine use scenario on the right is presented to account for changes observed in cocaine use disorder, including the decreased dopamine release previously observed with positron emission tomography (PET) and the increased neuromelanin-sensitive MRI (NM-MRI) signal reported here. A decrease in vesicular monoamine transporter 2 (VMAT2), also consistent with PET and postmortem studies, could account for both of these: decreased VMAT2 expression would decrease vesicular dopamine and increase the cytosolic dopamine pool from which neuromelanin is synthesized. (Please see the text for alternative interpretations of the data.)

vesicles and more dopamine in the cytosolic pool would explain the divergence between PET studies, which estimate dopamine release from vesicles, and imaging of NM, which accumulates on the basis of the concentration of dopamine in the cytosol (12, 26). If, on the other hand, cocaine use disorder were associated with a global and persistent decrease in dopamine synthesis, we would expect to have seen a decrease in both the PET and NM-MRI signals.

A number of previous studies support our hypothesis that cocaine use disorder involves a redistribution of dopamine between vesicular and cytosolic stores (Figure 3 is a graphical depiction of this hypothesis). Chronic cocaine exposure is associated with a reduction in vesicular monoamine transporter 2 (VMAT2) expression, which leads to less dopamine in the vesicular pool and more in the cytosolic pool. The reduction in VMAT2 has been shown in nonhuman primates who chronically self-administer cocaine (27) and in human cocaine users (28). Postmortem human

studies also show a reduction of striatal VMAT2 in cocaine users (29–31).

Blunted VMAT2 expression in cocaine use disorder would explain the decrease in presynaptic dopamine release seen with PET (1–4) and could also account for the decrease in [¹⁸F]DOPA accumulation seen in this population (32), since this likely depends on the radiotracer concentrating in synaptic vesicles (33). Reduced VMAT2 expression has also been shown to correlate with elevated NM formation in the midbrain (12, 34). While cocaine use has been shown to be associated with altered expression of dopamine receptors and transporters (1), likely including autoreceptors in the midbrain (35), these changes would generally shift both NM accumulation and dopamine release in the same direction. VMAT2 alteration, on the other hand, stands out as a parsimonious explanation for the observed changes occurring in opposing directions. Taken together, these imaging studies suggest that cocaine use is associated with lower dopamine in

the vesicular pool and a higher concentration in the cytosolic compartment. However, a study imaging VMAT2 and dopamine release in cocaine users combined with NM-MRI in the midbrain would be needed to confirm our hypothesis. If cocaine use indeed increases cytosolic dopamine, this may pose a risk to neurons, because oxidation of dopamine in this compartment forms reactive quinone species (36); however, there is no clear evidence of enhanced dopamine cell death (37) or Parkinson's disease risk (38) in cocaine users.

An alternative interpretation of our main finding is that NM elevation in cocaine users results from repeated episodic surges in dopamine that occurred over the participants' lifetime, which may not be captured by PET. Since NM granules are removed only after cell death (26), and thus serve as a long-term reporter of dopamine function, even a distant history of cocaine use (which may acutely lead to excess dopamine during cocaine consumption) could manifest as a persistent increase in the NM-MRI signal. Longitudinal studies would be needed to address this possibility.

As an initial test of the functional significance of our findings, we examined whether NM-MRI signal in cocaine-use voxels within the SN correlated with fMRI response to reward anticipation in the ventral striatum during the monetary incentive delay task, a robust probe of reward system function (15, 19, 25). We failed to find a significant correlation. This is perhaps unsurprising since the abnormality that we observed in cocaine users was not clustered near the "limbic" SN or ventral tegmental area (dorsomedial regions of our overinclusive SN mask [21]) that send the main projections to the ventral striatum. Rather, our topographical analysis showed that group differences predominated in the ventral (or "cognitive") SN (21), a subregion with prominent projections to the dorsal striatum thought to be involved in cognitive flexibility and other higher-order functions (20, 21). While PET imaging studies of dopamine function in cocaine users have found consistent evidence of dopaminergic alterations in the dorsal striatum, they have also found pronounced alterations in the ventral striatum (1). Intriguingly, our observation that cocaine users show an increase in NM-MRI signal in dorsal-striatum-projecting regions of the SN but not in ventral-striatum-projecting regions aligns with the previous observation of significant VMAT2 reductions in the dorsal but not the ventral striatum in this population (28, 31). Whatever may underlie this anatomical pattern, it highlights that nigrostriatal circuits subserving cognitive functions may be important in cocaine use disorder and that future studies may be better positioned to determine the functional significance of NM-MRI signal change in this disorder by probing higher-order cognitive processes in addition to reward tasks.

The primary limitation of this study is the relatively small, entirely male, sample. However, we contend that this first report of NM-MRI in substance use disorders supports the promise of this method for measuring dopamine function in this population. The only previous NM-MRI

study to investigate substance use was a preliminary evaluation of the size of the SN area in a small group of patients with psychotic illness. Psychotic patients with comorbid substance use exhibited a larger SN area than nonuser patients (39). We are not aware of previous work investigating NM concentration in postmortem tissue in substance use disorders, and this would be an important future direction to provide convergent support for our findings. Based on the present results, we cannot speak to the generalizability of our NM-MRI findings in cocaine users to other substance use disorders. Further research is needed to address this question, especially in light of our findings showing a near-significant relationship between NM-MRI and tobacco use (which may well reach significance in a larger sample or in heavier tobacco users). Assuming that increased NM signal is due to down-regulation of VMAT2 (27, 28), the reported NM-MRI phenotype may be specific to cocaine or other drugs affecting VMAT2 (perhaps including methamphetamine, although its relationship to VMAT2 is less clear [1]). The absence of a significant correlation between NM-MRI signal and duration of cocaine use in our data is surprising. Given that NM accumulates over time, we anticipated that longer duration of use would exaggerate any abnormalities observed in cocaine users. The lack of a significant relationship could, however, be due to the limited range in duration of use in our sample, as our participants had all been using cocaine for many years. The NM-MRI signal does not reflect a single biological process but could be altered by changes in dopamine synthesis (12), dopamine transfer to vesicles (34), or dopamine cell death (6). Such non-specificity is common to imaging measures (40, 41) and argues for the utility of multimodal studies in triangulating neurobiological mechanisms, as we have attempted to do by interpreting our findings in light of previous PET imaging reports. While interpretation of our NM-MRI results is simplified by the absence of enhanced dopamine cell death in cocaine users (37), interpretation of NM-MRI results in disorders showing substantial cell death combined with altered NM accumulation may be more challenging.

CONCLUSIONS

We have presented NM-MRI evidence for abnormal NM accumulation in cocaine users, an indirect indication of dopamine dysfunction consistent with previous work. Our work thus positions NM-MRI as a promising research tool for addiction and supports its development as a candidate biomarker for stimulant use disorders. Given the central role of dopamine in addiction and the ease of NM-MRI data acquisition, this method has the potential to advance our understanding of dopamine alterations in addiction, particularly as it affords the opportunity to study younger, at-risk populations and describe longitudinal trajectories of dopamine alterations, which has been challenging to do using PET.

AUTHOR AND ARTICLE INFORMATION

University of Ottawa Institute of Mental Health Research, affiliated with The Royal, Ottawa (Cassidy, Cheung); Department of Psychiatry, Columbia University College of Physicians and Surgeons, and New York State Psychiatric Institute, New York (Cassidy, Carpenter, Grasseti, Abi-Dargham, Martinez, Horga); Department of Psychiatry, Rutgers University, Piscataway, N.J. (Konova); Institute of Biomedical Technologies, National Research Council of Italy, Milan (Zecca); Department of Psychiatry, Stony Brook University, Stony Brook, N.Y. (Abi-Dargham). Send correspondence to Dr. Cassidy (clifford.cassidy@theroyal.ca).

Drs. Martinez and Horga contributed equally to this study.

Presented at the 57th annual meeting of the American College of Neuropsychopharmacology, Hollywood, Fla., December 9–13, 2018, and at the 74th annual meeting of the Society of Biological Psychiatry, Chicago, May 16–18, 2019.

Supported by NIDA grant R01 DA020855 (to Dr. Martinez and Carpenter) and by NIMH grants R01 MH117323 and R01 MH114965 (to Dr. Horga). Additional support was received from NIH's National Center for Advancing Translational Sciences through grant UL1TR001873.

The content is solely the responsibility of the authors and does not necessarily represent the official views of NIH.

Drs. Cassidy and Horga are inventors on a patent using the analysis method described here but have received no licensing fees or royalties. Dr. Abi-Dargham has served as a consultant for Otsuka, as an advisory board member for Sunovion, as a study section member for Neural Basis of Psychopathology, Addictions and Sleep Disorders Study Section, and as an associate editor for the Society of Biological Psychiatry and for the American College of Neuropsychopharmacology. The other authors report no financial relationships with commercial interests.

Received January 28, 2020; revisions received April 26 and June 17, 2020; accepted June 24, 2020; published online Aug. 28, 2020.

REFERENCES

- Ashok AH, Mizuno Y, Volkow ND, et al: Association of stimulant use with dopaminergic alterations in users of cocaine, amphetamine, or methamphetamine: a systematic review and meta-analysis. *JAMA Psychiatry* 2017; 74:511–519
- Martinez D, Carpenter KM, Liu F, et al: Imaging dopamine transmission in cocaine dependence: link between neurochemistry and response to treatment. *Am J Psychiatry* 2011; 168:634–641
- Martinez D, Narendran R, Foltin RW, et al: Amphetamine-induced dopamine release: markedly blunted in cocaine dependence and predictive of the choice to self-administer cocaine. *Am J Psychiatry* 2007; 164:622–629
- Volkow ND, Wang GJ, Fowler JS, et al: Decreased striatal dopaminergic responsiveness in detoxified cocaine-dependent subjects. *Nature* 1997; 386:830–833
- Cassidy CM, Zucca FA, Girgis RR, et al: Neuromelanin-sensitive MRI as a noninvasive proxy measure of dopamine function in the human brain. *Proc Natl Acad Sci USA* 2019; 116:5108–5117
- Sulzer D, Cassidy C, Horga G, et al: Neuromelanin detection by magnetic resonance imaging (MRI) and its promise as a biomarker for Parkinson's disease. *NPJ Parkinsons Dis* 2018; 4:11
- Zecca L, Fariello R, Riederer P, et al: The absolute concentration of nigral neuromelanin, assayed by a new sensitive method, increases throughout the life and is dramatically decreased in Parkinson's disease. *FEBS Lett* 2002; 510:216–220
- Trujillo P, Summers PE, Ferrari E, et al: Contrast mechanisms associated with neuromelanin-MRI. *Magn Reson Med* 2017; 78:1790–1800
- Zecca L, Bellei C, Costi P, et al: New melanic pigments in the human brain that accumulate in aging and block environmental toxic metals. *Proc Natl Acad Sci USA* 2008; 105:17567–17572
- Martín-Bastida A, Lao-Kaim NP, Roussakis AA, et al: Relationship between neuromelanin and dopamine terminals within the Parkinson's nigrostriatal system. *Brain* 2019; 142:2023–2036
- Watanabe Y, Tanaka H, Tsukabe A, et al: Neuromelanin magnetic resonance imaging reveals increased dopaminergic neuron activity in the substantia nigra of patients with schizophrenia. *PLoS One* 2014; 9:e104619
- Sulzer D, Bogulavsky J, Larsen KE, et al: Neuromelanin biosynthesis is driven by excess cytosolic catecholamines not accumulated by synaptic vesicles. *Proc Natl Acad Sci USA* 2000; 97:11869–11874
- Cebrián C, Zucca FA, Mauri P, et al: MHC-I expression renders catecholaminergic neurons susceptible to T-cell-mediated degeneration. *Nat Commun* 2014; 5:3633
- McCutcheon RA, Abi-Dargham A, Howes OD: Schizophrenia, dopamine, and the striatum: from biology to symptoms. *Trends Neurosci* 2019; 42:205–220
- Oldham S, Murawski C, Fornito A, et al: The anticipation and outcome phases of reward and loss processing: a neuroimaging meta-analysis of the monetary incentive delay task. *Hum Brain Mapp* 2018; 39:3398–3418
- Urban NB, Slifstein M, Meda S, et al: Imaging human reward processing with positron emission tomography and functional magnetic resonance imaging. *Psychopharmacology (Berl)* 2012; 221:67–77
- Schott BH, Minuzzi L, Krebs RM, et al: Mesolimbic functional magnetic resonance imaging activations during reward anticipation correlate with reward-related ventral striatal dopamine release. *J Neurosci* 2008; 28:14311–14319
- Luijten M, Schellekens AF, Kühn S, et al: Disruption of reward processing in addiction: an image-based meta-analysis of functional magnetic resonance imaging studies. *JAMA Psychiatry* 2017; 74:387–398
- Balodis IM, Potenza MN: Anticipatory reward processing in addicted populations: a focus on the monetary incentive delay task. *Biol Psychiatry* 2015; 77:434–444
- Weinstein JJ, Chohan MO, Slifstein M, et al: Pathway-specific dopamine abnormalities in schizophrenia. *Biol Psychiatry* 2017; 81:31–42
- Zhang Y, Larcher KM, Masic B, et al: Anatomical and functional organization of the human substantia nigra and its connections. *eLife* 2017; 6:e26653
- Zimet GD, Dahlem NW, Zimet SG, et al: The multidimensional scale of perceived social support. *J Pers Assess* 1988; 52:30–41
- Beck AT, Steer RA, Ball R, et al: Comparison of Beck Depression Inventories-IA and -II in psychiatric outpatients. *J Pers Assess* 1996; 67:588–597
- Andrews MM, Meda SA, Thomas AD, et al: Individuals family history positive for alcoholism show functional magnetic resonance imaging differences in reward sensitivity that are related to impulsivity factors. *Biol Psychiatry* 2011; 69:675–683
- Wu CC, Samanez-Larkin GR, Katovich K, et al: Affective traits link to reliable neural markers of incentive anticipation. *Neuroimage* 2014; 84:279–289
- Zucca FA, Basso E, Cupaioli FA, et al: Neuromelanin of the human substantia nigra: an update. *Neurotox Res* 2014; 25:13–23
- Narendran R, Jedema HP, Lopresti BJ, et al: Decreased vesicular monoamine transporter type 2 availability in the striatum following chronic cocaine self-administration in nonhuman primates. *Biol Psychiatry* 2015; 77:488–492
- Narendran R, Lopresti BJ, Martinez D, et al: In vivo evidence for low striatal vesicular monoamine transporter 2 (VMAT2) availability in cocaine abusers. *Am J Psychiatry* 2012; 169:55–63
- Little KY, Krolewski DM, Zhang L, et al: Loss of striatal vesicular monoamine transporter protein (VMAT2) in human cocaine users. *Am J Psychiatry* 2003; 160:47–55
- Little KY, Zhang L, Desmond T, et al: Striatal dopaminergic abnormalities in human cocaine users. *Am J Psychiatry* 1999; 156:238–245

31. Wilson JM, Levey AI, Bergeron C, et al: Striatal dopamine, dopamine transporter, and vesicular monoamine transporter in chronic cocaine users. *Ann Neurol* 1996; 40:428–439
32. Wu JC, Bell K, Najafi A, et al: Decreasing striatal 6-FDOPA uptake with increasing duration of cocaine withdrawal. *Neuropsychopharmacology* 1997; 17:402–409
33. Kumakura Y, Cumming P: PET studies of cerebral levodopa metabolism: a review of clinical findings and modeling approaches. *Neuroscientist* 2009; 15:635–650
34. Liang CL, Nelson O, Yazdani U, et al: Inverse relationship between the contents of neuromelanin pigment and the vesicular monoamine transporter-2: human midbrain dopamine neurons. *J Comp Neurol* 2004; 473:97–106
35. Worhunsky PD, Matuskey D, Gallezot JD, et al: Regional and source-based patterns of [¹¹C]-(+)-PHNO binding potential reveal concurrent alterations in dopamine D₂ and D₃ receptor availability in cocaine-use disorder. *Neuroimage* 2017; 148:343–351
36. Segura-Aguilar J, Paris I, Muñoz P, et al: Protective and toxic roles of dopamine in Parkinson's disease. *J Neurochem* 2014; 129:898–915
37. Bennett BA, Hyde CE, Pecora JR, et al: Long-term cocaine administration is not neurotoxic to cultured fetal mesencephalic dopamine neurons. *Neurosci Lett* 1993; 153:210–214
38. Asser A, Taba P: Psychostimulants and movement disorders. *Front Neurol* 2015; 6:75
39. Tavares M, Reimão S, Chendo I, et al: Neuromelanin magnetic resonance imaging of the substantia nigra in first episode psychosis patients consumers of illicit substances. *Schizophr Res* 2018; 197: 620–621
40. Guo N, Hwang DR, Lo ES, et al: Dopamine depletion and in vivo binding of PET D1 receptor radioligands: implications for imaging studies in schizophrenia. *Neuropsychopharmacology* 2003; 28: 1703–1711
41. Logothetis NK: What we can do and what we cannot do with fMRI. *Nature* 2008; 453:869–878